Assessment of atmospheric reductions for terrestrial gravity observations

M.Abe[1], C.Kroner[1], J.Neumeyer, X.D. Chen[2]

1) Deutsches GeoForschungsZentrum (GFZ), Gravity Field and Gravimetry
2) Institute of Geodesy and Geophysics, Chinese Academy of Sciences

Abstract

Atmospheric attraction and loading effects account for about 10% of all observed time-dependent gravity variations in which the dominant gravity signal is the tides of the solid Earth. The impact can be roughly estimated using barometric pressure from the observation site, but in that case only atmospheric variations which are correlated with local barometric pressure changes are taken into account. If e.g. geodynamic signals are to be investigated, the variations which are unconsidered have an amplitude of several μGal, therefore they are large enough to require consideration.

In this paper, three different procedures to remove the atmospheric effect are compared. Numerical results show that the atmospheric reduction using three-dimensional (3D) data from the European Center for Medium-Range Weather Forecasts (ECMWF) ought to be computed up to 5° around a station. A peak-to-peak amplitude of the differences between a reduction using 3D data and one using two-dimensional (2D) data from the ECMWF is 0.5 μGal including seasonal variations with an amplitude of 0.15 μGal, and it has a Root Mean Square (RMS) value of 0.1 μGal considering a time span of 4 years. The amplitude of reduction based on a regression coefficient/admittance factor differs from the two physical methods by approximately 3 μGal with a RMS value of 0.4 μGal in the same 4 year-long observation period.

From spectral analyses of the three reductions it emerges that the amplitudes of the more comprehensive methods are 11-12% smaller than the reduction using an admittance factor in the spectral range from 0.0 CPD (cycle per day) to 0.18 CPD on average. Investigation of the atmospheric reduction effects on the tidal analysis indicates that there are visible improvements in the tidal analysis using the reductions based on the physical approaches compared to the reduction using an admittance factor but not between the two physical approaches. Concerning the amplitude factor of the polar motion signal, there is 1.5% difference in the value of the factor after applying the two physical methods.

The differences between the physical approaches stem from the consideration of the air density distribution. A peak-to-peak amplitude is about 0.5 μGal when the attraction effect up to 5° around a station is computed. The omission of vertical variations in air density leads to inaccuracies which should be avoided, for instance, in the validation of non-tidal ocean loading effects or studies of tectonic phenomena.

Keywords: Atmospheric reduction, Time variable gravity

1. Introduction

The estimation of atmospheric attraction and loading effects are necessary for continuous and precise gravity observations, e.g., with superconducting gravimeters (SG), because gravity variations induced by shifts of air masses cover geodynamic signals of interest. Therefore, this atmospheric impact should be modeled as well as possible and be removed from the gravity observations.

A still widely used atmospheric reduction is based upon an admittance factor adjusted by least square fitting between barometric pressure and SG data from an observation site. By using this method, however, only effects which are correlated with local pressure are taken into account and effects uncorrelated are not considered.

During the recent past, several attempts were made (e.g. Merriam, 1992; Sun et al. 1995; Boy et al., 1998, 2002; Kroner & Jentsch, 1999; Guo et al., 2004) to improve reductions by means of Green's functions (Farrell, 1972) or using an empirical frequency-dependent method (Warburton & Goodkind, 1977; Crossley et.al., 1995; Neumeyer, 1995).

Merriam (1992) calculated atmospheric Green's functions (attraction and deformation), which are based on the ideal gas law, the hydrostatic assumption, and a temperature model of the COSPAR (Committee on Space Research) atmosphere. These are computed over a thin column from a height from 0 to 60 km. The attraction and loading effect can be computed from these functions and surface barometric pressure data for the whole Earth. As here only surface pressure is considered, surface pressure independent air mass movements are not taken into account.

Neumeyer et al. (2004) computed a physical reduction using three-dimensional (3D) meteorological model data from the European Center for Medium-Range Weather Forecasts (ECMWF). The attraction effect was calculated up to 1.5° distance from the SG station and for the deformation part using Green's function a distance up to 10° was considered. The amplitude of the attraction part which does not correlate with barometric pressure observed at the Earth's surface was about 2.0 μGal (Neumeyer et al., 2006).

The present investigation is based on the studies by Neumeyer et al. (2004, 2006) and the object of this paper is to derive an optimized atmospheric reduction suitable for ongoing research related to gravity changes of several days and longer (e.g. related polar motion or non-tidal ocean loading etc.). Thus, in this study the focus is atmospheric variations with spatial scales of tens of kilometers to global. Reductions for atmospheric effects are a means to an end, because gravity data interpretation begins after the atmospheric reduction. In this paper, we determine how large the zone needs to be for the computation of the attraction effect using 3D meteorological data and from which distance it is sufficient to use surface data and a standard atmosphere. We use spectral and tidal analyses to investigate and quantify the differences between the various reduction methods.

2. Data and method

2-1 The ECMWF data

7 data sets (surface geopotential, surface pressure, 2 m temperature, humidity with 60/90 height levels, temperature with 60/90 height levels, geopotential with 60/90 height levels, and barometric pressure with 60/90 height levels) from ECMWF Integrated Forecast System (IFS) daily analysis and error estimates are used in this investigation. The original data are re-sampled to a regular grid of 0.5° × 0.5° and the coverage is 89.5° to - 89.5° in latitude and 0° to 359.5° in longitude. The sampling rate is 6 h. Until 31.01.2006, ECMWF provided data for 60 height levels (about up to 64 km height), after this date the number of height levels was increased to 91 (about 80 km height). The gravity effects due to this modification amount to 8.42×10^{-4} μGal in a time span of 11 months. These effects are therefore small enough to be ignored in this study.

2-2 The air density distribution

For the estimation of the atmospheric attraction term, the air density distribution needs to be computed for each cell of air mass.

The atmosphere is considered as a mixture of dry air and water vapor. By using the ideal gas equation the air density ρ can be derived from

$$\rho = \frac{p}{RT(1-q+\frac{q}{\varepsilon})} \quad (1),$$

where R is the gas constant for dry air ($287.05\,Jkg^{-1}K^{-1}$), p, q, T are respectively barometric pressure, humidity, temperature taken from ECMWF data (from the Earth's surface to 80 km height) and ε is the ratio of the gas constants for dry air R and water vapour R_v ($\varepsilon = \frac{R}{R_v} = 0.62197$). Fig. 1a shows the air density distribution using (1) and ECMWF data for the example of Moxa station (Fig.3)(50.6447° N, 11.6156° E and a height of 455m) for the time span of one month and the vertical density distribution derived from the U.S. Standard Atmosphere 1976 (NASA,1976) and the well-known barometric formula (2)

$$\rho(z) = \frac{P_0}{RT_Z}\left(\frac{T_0+\alpha z}{T_0}\right)^{-\frac{g_0}{R\alpha}} \quad (2)$$

with $T_Z = T_0 + \alpha z$ and α as the rate of temperature change with height from the US1976 standard atmosphere up to 84 km. P_0 and T_0 are respectively surface pressure and temperature from ECMWF, T_Z is temperature at height z, and g_0 is the mean surface gravity value 9.80665 m/s^2.

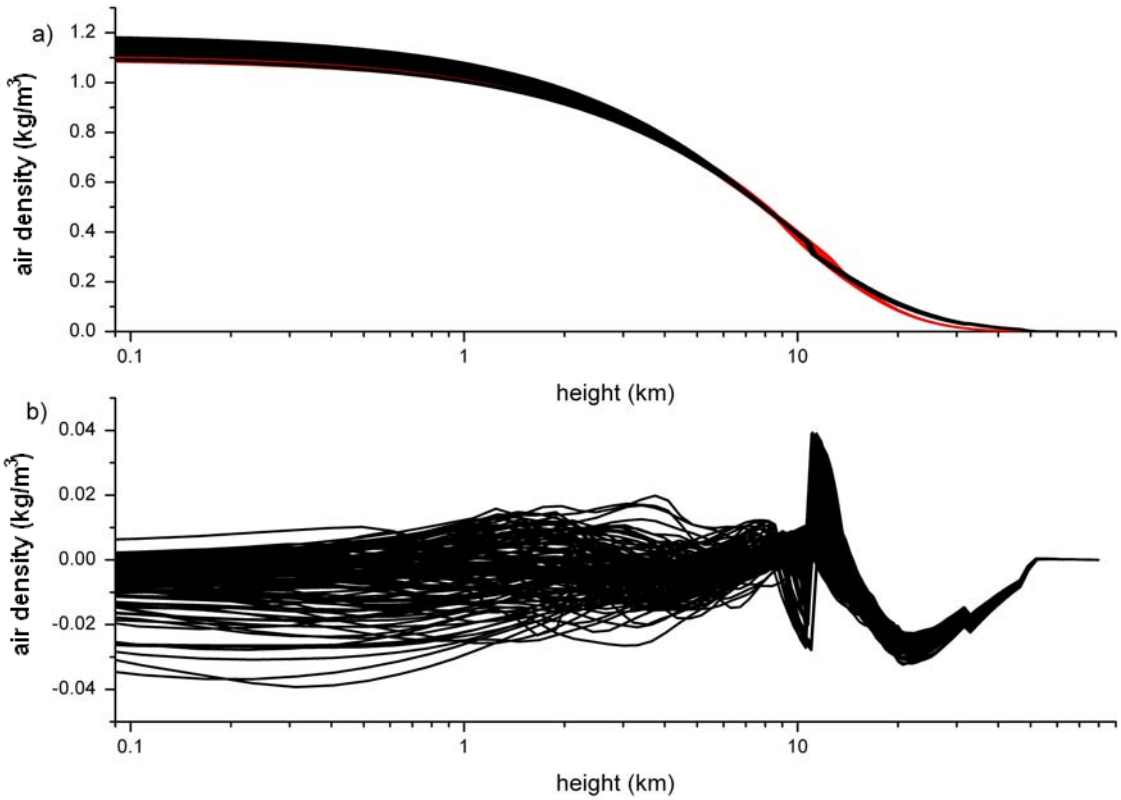

Figure 1
Air density distributions for Moxa station from 2007/07/01-2007/07/31
(a) red line : ECMWF data , black line : The US 1976 standard atmosphere
(b) difference (air density derived from ECMWF data – US standard atmosphere)

The air density distribution is computed from 1st of July, 2007 to 31st of July, 2007. In Fig.1b the difference between the air density distribution based on eq.(2) and 3D ECMWF data is shown. Random variations occur up to a height of 10 km with a deviation range of -0.04 to 0.02 kg/m^3. The differences become larger up to 0.04 kg/m^3 in a height of 11 km. Between 11 and 20 km distinct deviations are found. From the height of 20 km or more, the differences approach gradually 0. In Neumeyer et al. (2004), a test calculation was carried out to estimate how much the changes in the air density profiles affect the gravity reduction. Air density profiles were changed within the range of 0.02 kg/m^3 up to 16km height and during 5 h. From this test calculation, gravity changes of about 3 μGal were obtained.
Thus, the deviation range of -0.04 to 0.02 kg/m^3 induces non-negligible gravity variations.

2-3 Calculation of the attraction term using 3D data

The calculation of the attraction term using 3D data is based on the gravitational potential of the air masses. Using spherical coordinates (λ, ϑ, r) with origin at the centre of the Earth and the Z-axis coinciding with the observation station, the gravitational potential of the air mass Φ is given by

$$\Phi(0,0,R_{GS}) = -\gamma \int_{R_{GS}}^{\infty} \int_{0}^{\pi} \int_{0}^{2\pi} \frac{\rho(\lambda,\vartheta,r)\cdot r^2 \sin\vartheta}{\sqrt{r^2 - 2rR_{GS}\cos\vartheta + R_{GS}^2}}\, d\lambda d\vartheta dr \quad (3),$$

where γ is the gravitational constant, R_{GS} is the radius of the Earth and ρ is the air density.

The gravitational potential of each air segment is changed to the gravitational acceleration caused by one spherical segment in the direction of the center of the mass

$$g_i^{\Delta}(0,0,R_{GS}) = -\frac{\partial}{\partial R_{GS}} \Phi_i^{\Delta} = \gamma \int_r \int_{\vartheta} \int_{\lambda} \frac{\partial}{\partial R_{GS}} \left(\frac{\rho_i r^2 \sin\vartheta}{\sqrt{r^2 - 2rR_{GS}\cos\vartheta + R_{GS}^2}} \right) d\lambda d\vartheta dr \quad (4).$$

Equation (4) is differentiated, and becomes

$$g_i^{\Delta}(0,0,R_{GS}) = -\gamma \int_r \int_{\vartheta} \int_{\lambda} \frac{\rho_i r^2 \sin\vartheta (R_{GS} - r\cos\vartheta)}{(r^2 - 2rR_{GS}\cos\vartheta + R_{GS}^2)^{\frac{3}{2}}} d\lambda d\vartheta dr \quad (5).$$

The total acceleration of all spherical air segments is obtained by solving equation (5) and summing up all contributions. Detailed explanations can be found in Neumeyer et al. (2004, 2006).

As is well known, the atmospheric attraction effect is strongly dependent on the distance. Thus, in the vicinity of a station a large effect exists, so that it is not sufficient to use the 0.5° ×0.5° spacing of the ECMWF data. According to Neumeyer et al., (2004, 2006), therefore air density values are interpolated by means of bi-linear interpolation. 42 additional grid points are computed in the zone between 0 and 0.5°. This means the attraction effect can be calculated every 0.0119° in this zone.

2-4 Calculation of the attraction and deformation effect using 2D data and atmospheric Green's functions

The surface pressure data provided by ECMWF are also used for the calculation of the deformation and the attraction effect based on the formula given in Merriam (1992). The attraction part thus obtained is compared with the variation derived from 3D data.

The attraction and deformation terms at angular distance ϕ from the base of a column of air with an area A in steradians are given by

$$g(\phi)^{deformation} = \frac{GE(\phi)}{10^5 \phi(rad)} \frac{A}{2\pi\left[1 - \cos(1^\circ)\right]} \mu Gal/hPa \quad (6)$$

$$g(\phi)^{attraction} = \frac{GN(\phi)}{10^5 \phi(rad)} \frac{A}{2\pi\left[1 - \cos(1^\circ)\right]} \mu Gal/hPa \quad (7).$$

$GE(\phi)$ and $GN(\phi)$ are respectively the elastic deformation term and Newtonian attraction term from Merriam (1992, Table1 The atmospheric load gravity functions). For the oceans an inverted barometer response is assumed.

We investigate also effects of temperature variations for the calculation of the attraction effect using 2D data. According to the Merriam (1992), when the

temperature effect is considered, the tabular expression for $GN(\phi)$ should be modified in the following way:

$$GN(\phi) = GN(\phi)_{table} + \frac{\partial GN}{\partial T}(T_0 - 15°C) \quad (8)$$

T_0 is the surface temperature. Fig.2 shows the difference between the atmospheric reduction using 2D data with and without temperature variations.

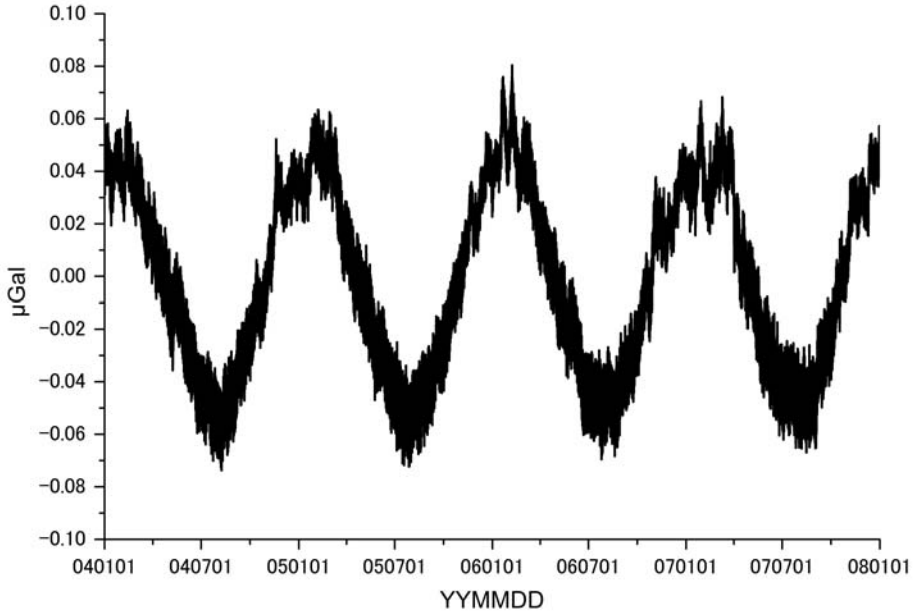

Figure 2
Differences between the attraction effects with and without temperature variation for the reduction using 2D data in Moxa from 2004/01/01 to 2007/12/31 (reduction using (2D with temperature)data – reduction using 2D data)

The peak-to-peak amplitude of the difference between both 2D reductions is 0.14 μGal with a dominant seasonal component and it has a RMS value of 0.036 μGal considering a time span of 4 years.

3. Results

3-1 Comparison between the reductions based on 2D and 3D data

To develop an optimized barometric pressure reduction suitable for current research related to gravity changes of several days and longer, we investigate how spatially extensive the zone needs to be for which the attraction effect should be computed using 3D data sets. This is done by computing the 3D atmospheric attraction effect around the Moxa station up to 15 ° for 6 zones (Fig.3), respectively the zone from the station to 0.5°, and the ring-shape zone from 0.5° to 1.5°, from 1.5° to 3°, from 3° to 5°, from 5° to 10°, and from 10° to 15°.

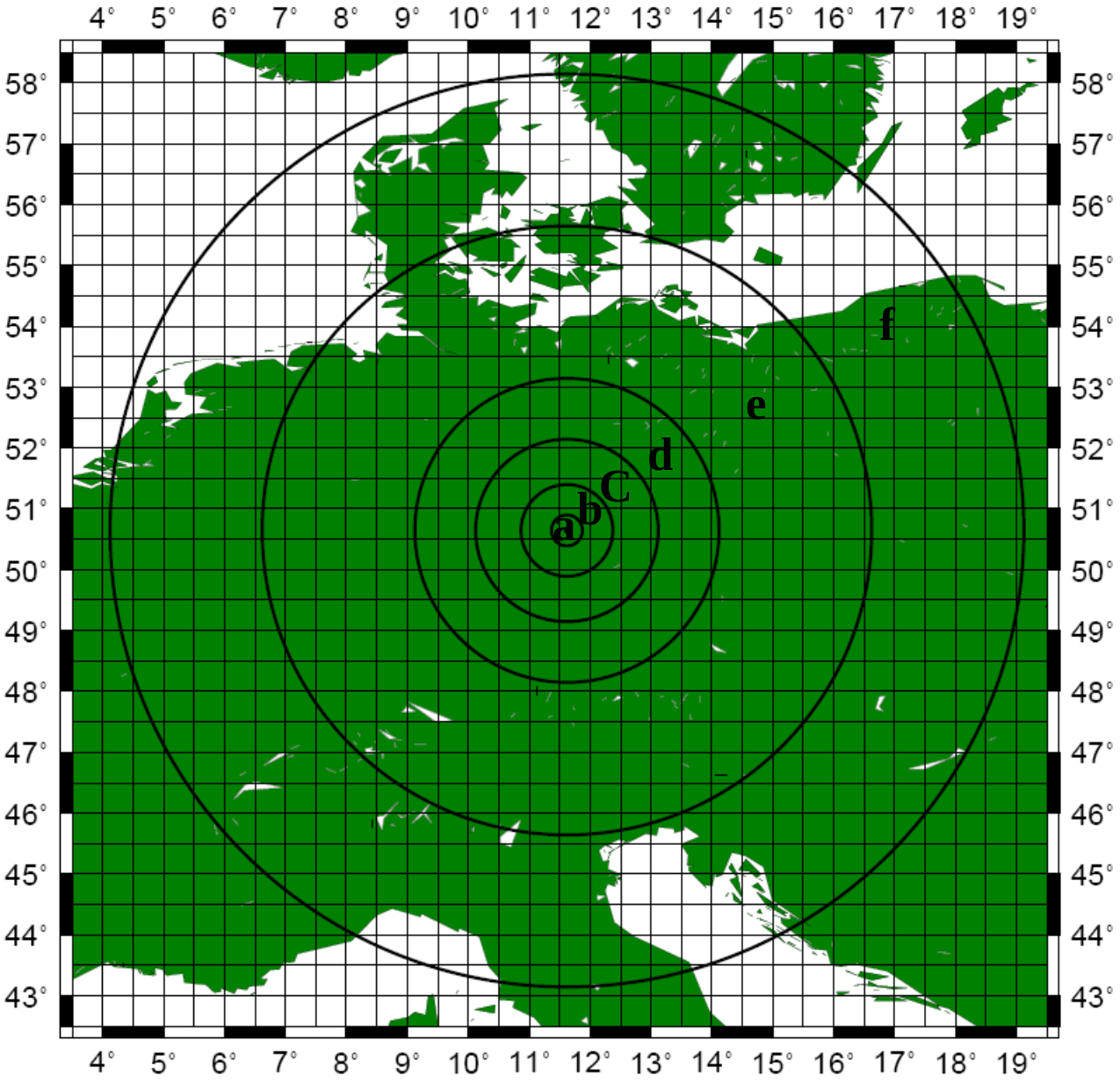

Figure 3
Location of Moxa station and considered zones
a) up to 0.5° , b) 0.5° - 1.5°, c) 1.5°-3°, d) 3°-5°, e) 5°-10°, f) 10°-15°

Fig.4 shows the atmospheric attraction using 3D data for one year from each zone.

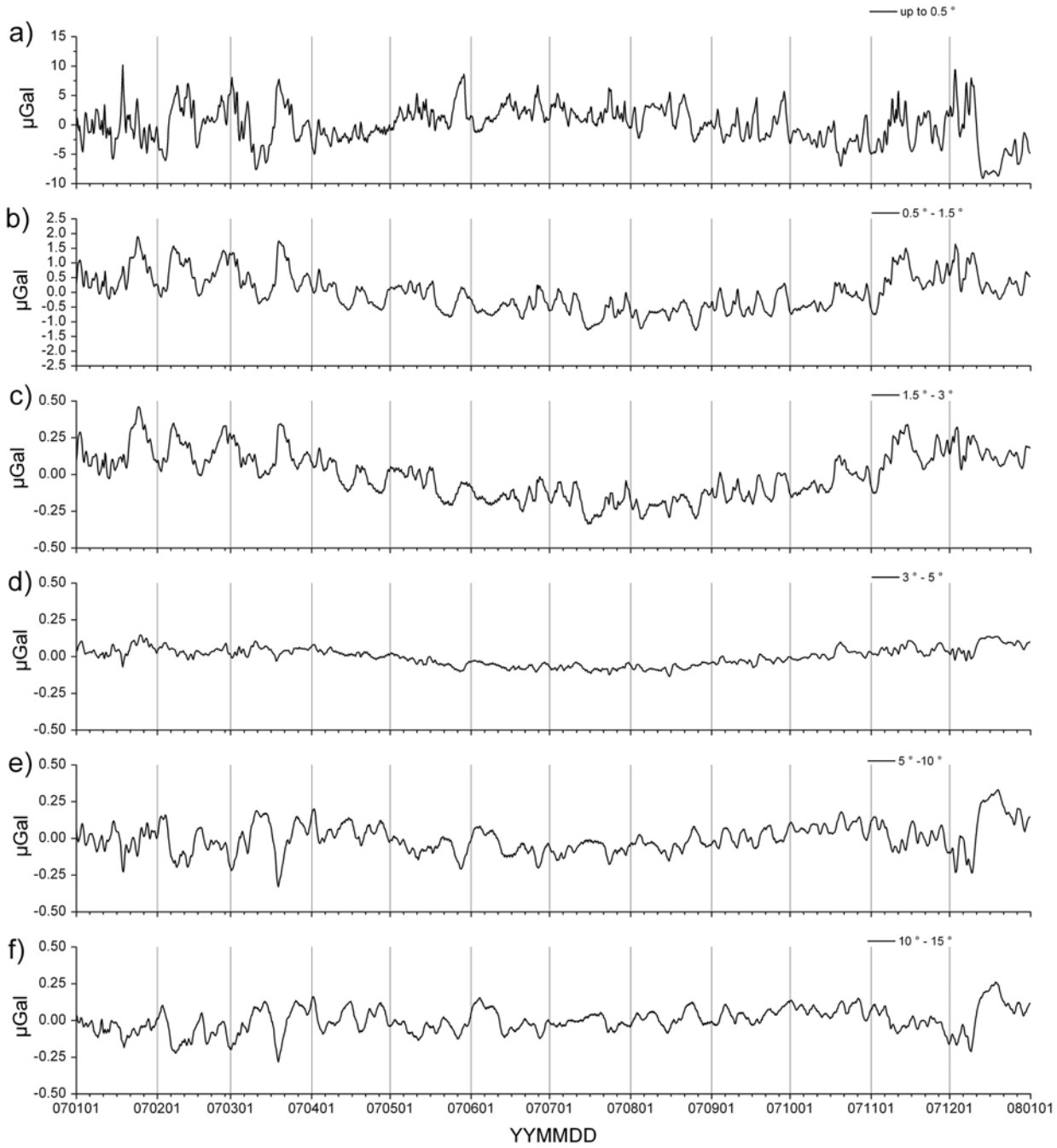

Figure 4
Attraction effect from the zones indicated in Fig.2 computed with 3D data from 2007/01/01 to 2007/12/31 (different scaling)
a) up to 0.5° , b) 0.5°- 1.5° , c) 1.5°- 3.0° , d) 3.0°- 5.0° , e) 5.0° - 10.0° , e) 10.0°- 15.0°

For the innermost zone the maximal amplitude of attraction effect is around 20 µGal and the Root Mean Square (RMS) value is 3.19 µGal. The peak-to-peak effect from the zone of 0.5° - 1.5° is roughly 1/7 of the innermost zone and the contribution from the zone of 1.5° - 3° reaches 1/30 of the innermost zone. The amplitude of the attraction effect from the zone of 3° - 5° has a peak-to-peak amplitude of 0.3 µGal (Fig.6d), a RMS value of 0.06 µGal and the effect from this zone is the smallest one. The variations from the zone of 5° - 10° and 10° - 15°

revert in sign. The reason for this is that due to the Earth's curvature, the attraction effect around the zone of 3° - 5° is nearly at the same height level as the gravity meter. The attraction from the zone which is more than 5° from the gravity station is already below the height level of the gravity meter. Thus, the direction of the attraction effect changes in sign. These characteristics are also visible in the tabulated Green's functions in Merriam (1992).

In order to estimate for which area the attraction effect using 3D data should be computed, a reduction based on 2D surface data (pressure and temperature) from ECMWF and a standard atmosphere is calculated for comparison (Fig.5).

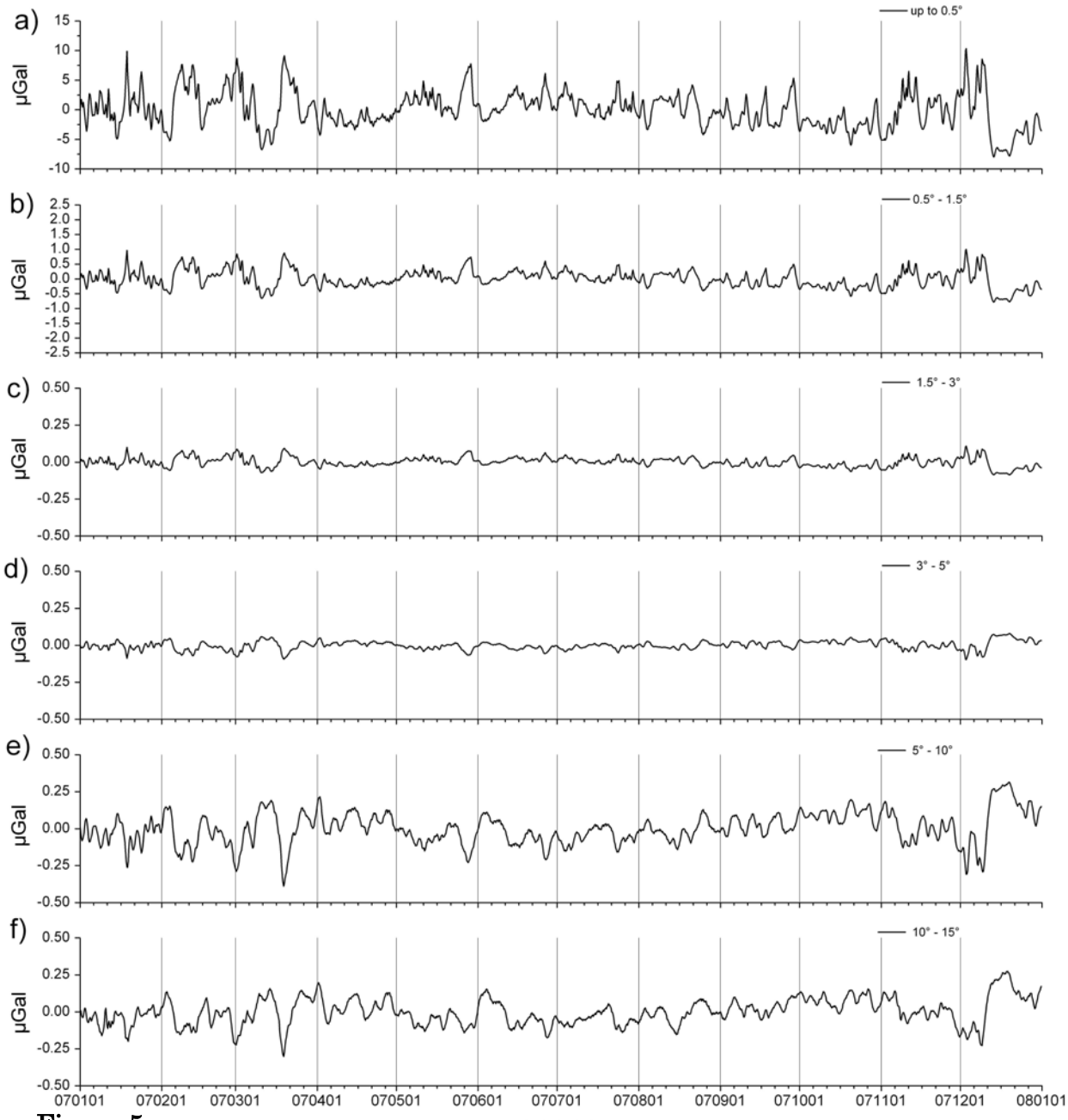

Figure 5

Attraction effect from the zones indicated in Fig.2 computed with 2D with temperature data from 2007/01/01 to 2007/12/31 (different scaling)

a) up to 0.5° , b) 0.5°- 1.5° , c) 1.5°- 3.0° , d) 3.0°- 5.0° , e) 5.0° - 10.0° , e) 10.0°- 15.0°

The attraction effect using 2D data from the innermost zone has an amplitude of 18 µGal and a RMS value of 3.0 µGal. The attraction effect from the zone of 0.5° - 1.5° is 10 times smaller than that of the innermost zone. Moreover the impact of the zone of 1.5° - 3° is 100 times smaller than the innermost zone and this variation is 3 times smaller than the variation calculated using 3D data. The variations from the remaining zones have similar features as the effect based on 3D data.

The differences between the gravity reductions using 3D data and 2D data are given for one year in Fig. 6.

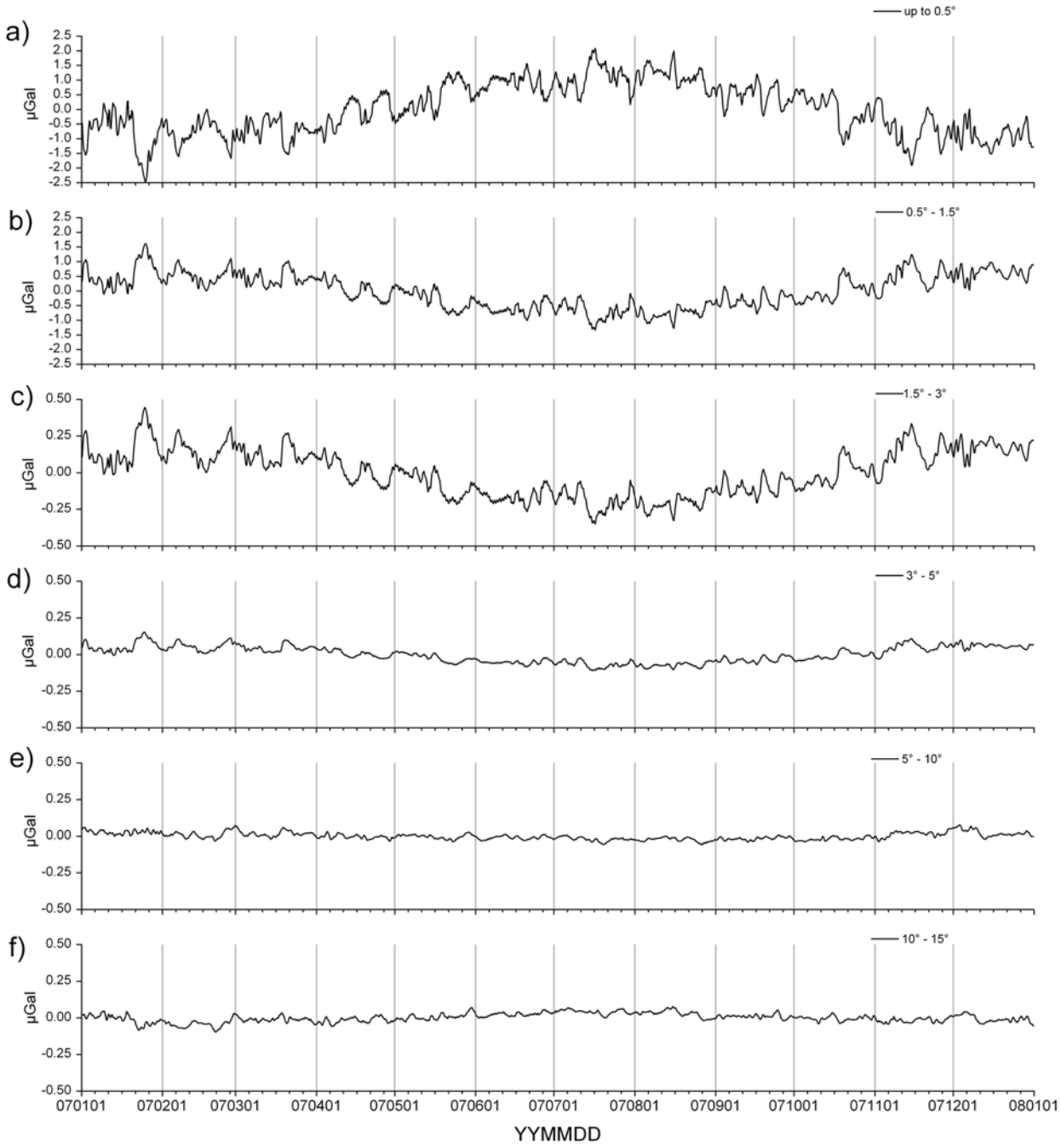

Figure 6
Differences between the attraction effects derived from 3D data and 2D with temperature data for zones of
a) up to 0.5° , b) 0.5° - 1.5°, c) 1.5°-3°, d) 3°-5°, e) 5°-10°, f) 10°-15° from 2007/01/01 to 2007/12/31 (different scaling)

It shows also the gravity effect of the surface pressure independent (SPI) part caused by the mass redistribution within the atmosphere from each zone. For the zone up to 0.5° (Fig.6a), the differences are in the range of 4.5 µGal with a maximum in summer and have a RMS value of 0.88 µGal. The differences for the zones 0.5° - 1.5° and 1.5° - 3° have a peak-to-peak amplitude of 3 µGal and 0.8 µGal (Fig.6b, c) and a minimum in summer. RMS values are 0.58 µGal and 0.16 µGal. As mentioned before, in these areas, the amplitude of the attraction effect using 3D data is 2-3 times larger than the effect obtained from 2D data. Thus, the differences show variations similar to the attraction effect using 3D data. The differences for the zone of 3° - 5° , 5° - 10° and 10°- 15° (Fig.6d,e,f) reach a peak-to-peak amplitude of 0.26 µGal, 0.14 µGal, and 0.18 µGal and RMS values are 0.05 µGal, 0.02 µGal and 0.03 µGal. The differences for the zone larger than 5° are below 0.2 µGal. This is two orders of magnitude smaller values than the total atmospheric effect. Therefore it is concluded that it is sufficient to use 3D data up to 5° and to compute the attraction effect for the remaining earth's surface from 2D data and atmospheric Green's functions. Up to the zone of 5°, there is a peak-to-peak difference of 0.5 µGal including seasonal variations with an amplitude of 0.15 µGal. The RMS value is 0.1 µGal considering a time span of 4 years (Fig.8a). The difference between the 3D and 2D data sets becomes smaller if we sum up the atmospheric attraction effect from each zone.

3-2 Comparison with 3 different atmospheric reductions

In order to gain insight on where the various pressure reductions differ, the three reductions are compared again for the example of Moxa station. Reductions comprise a) 3D data for an area up to 5° to calculate the atmospheric attraction effect, 2D data (pressure and temperature) for the rest of the Earth to calculate the atmospheric attraction effect and 2D data for the whole Earth to calculate the atmospheric loading effect (physical approach), b) 2D data (pressure and temperature) for the whole Earth for the calculation of the atmospheric attraction and loading effect (physical approach), c) an admittance factor (-0.3649 µGal/hPa) which is estimated from the regression analysis between observed barometric pressure data and SG data (standard method). Fig.7 shows these reductions for a time span of 4 years.

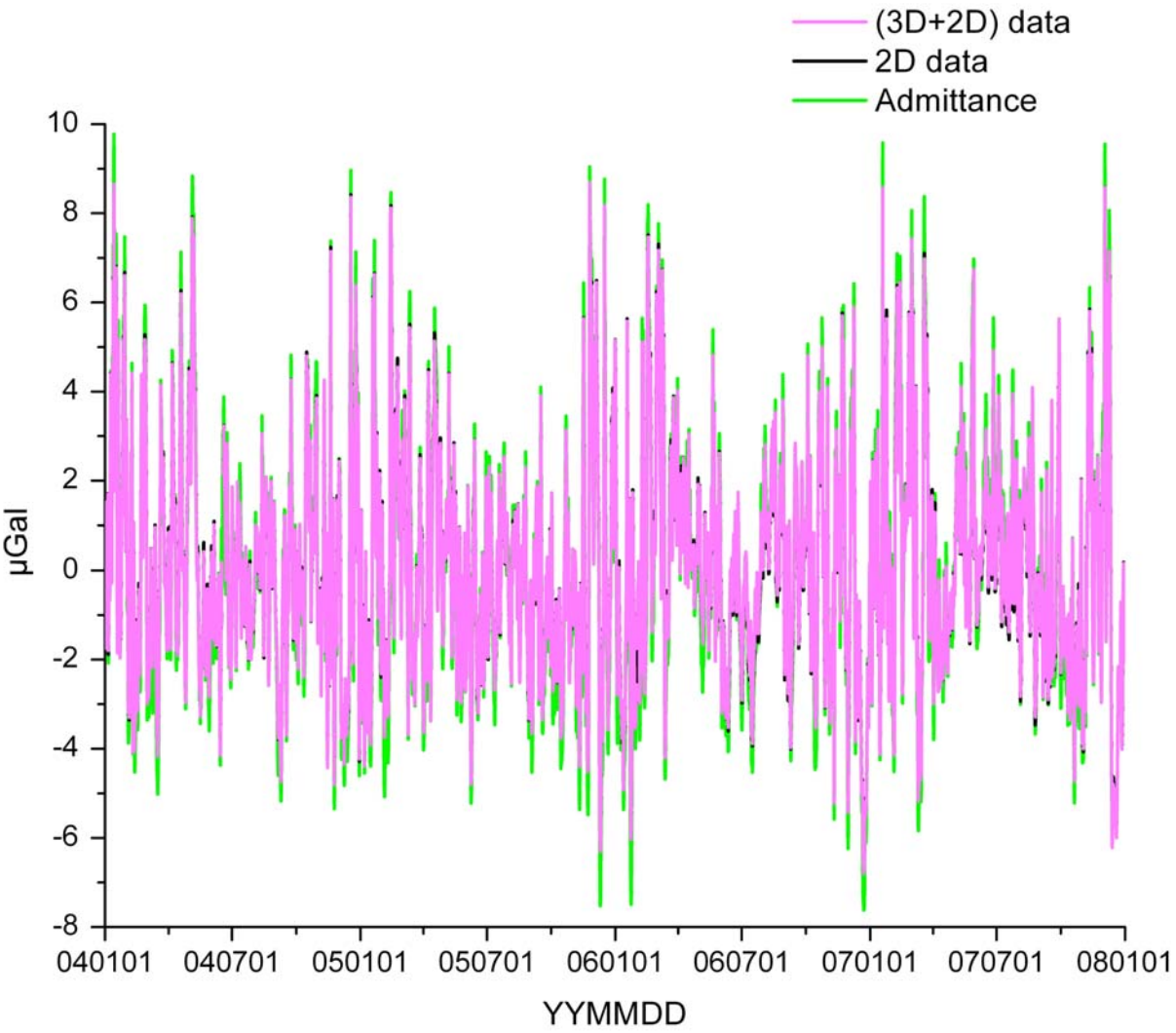

Figure 7
Atmospheric reductions for Moxa observatory from 2004/01/01 to 2007/12/31
(3D+2D) data =
attraction effect : based on 3D data up to 5 degree around station + 2D data are used for the calculation of the rest of the Earth
deformation effect : based on 2D data
2D data = attraction and deformation effect : based on 2D data
Admittance = the reduction based on admittance factor

The reduction using an admittance factor is larger than the others. The difference between the reductions is given in Fig.8 for the same 4 year-long data set.

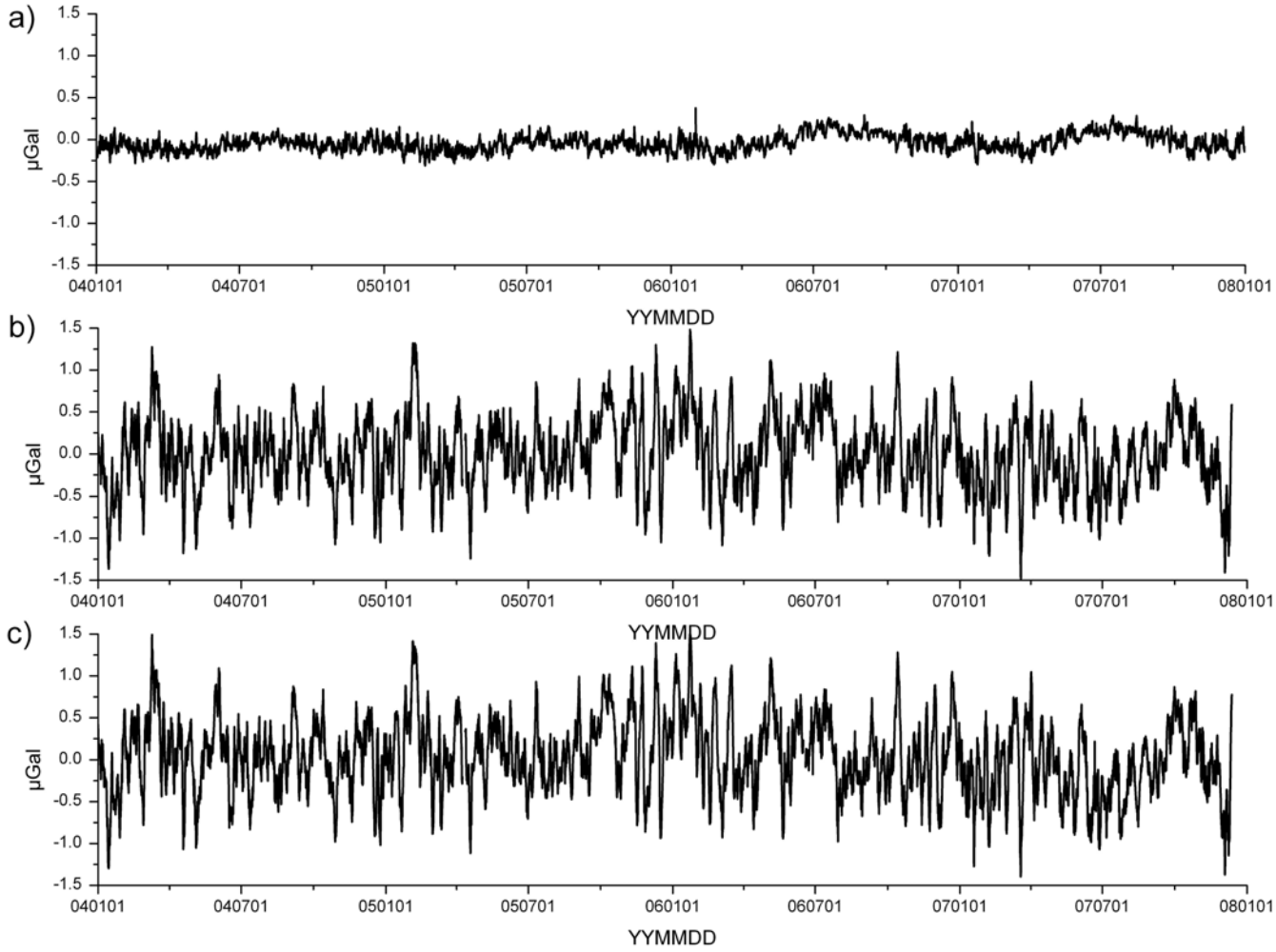

Figure 8
Differences between atmospheric reductions from 2004/01/01 to 2007/12/31
a) based on 3D+2D data - 2D data
b) based on 3D+2D - admittance factor
c) based on 2D data - admittance factor

The difference between the two reductions based on a physical approach (Fig.8a) has a peak-to-peak amplitude of 0.5 µGal including seasonal variations with an amplitude of 0.15 µGal as mentioned previously with a maximum in summer. The RMS value amounts to 0.1 µGal. Fig.8b, c show respectively the differences between the reductions derived from the two physical approaches and an admittance factor. They have similar variations and a peak-to-peak amplitude of 3 µGal with a RMS value of 0.4 µGal.

In order to determine, in which spectral ranges the differences occur, spectral analyses are computed (Fig.9).

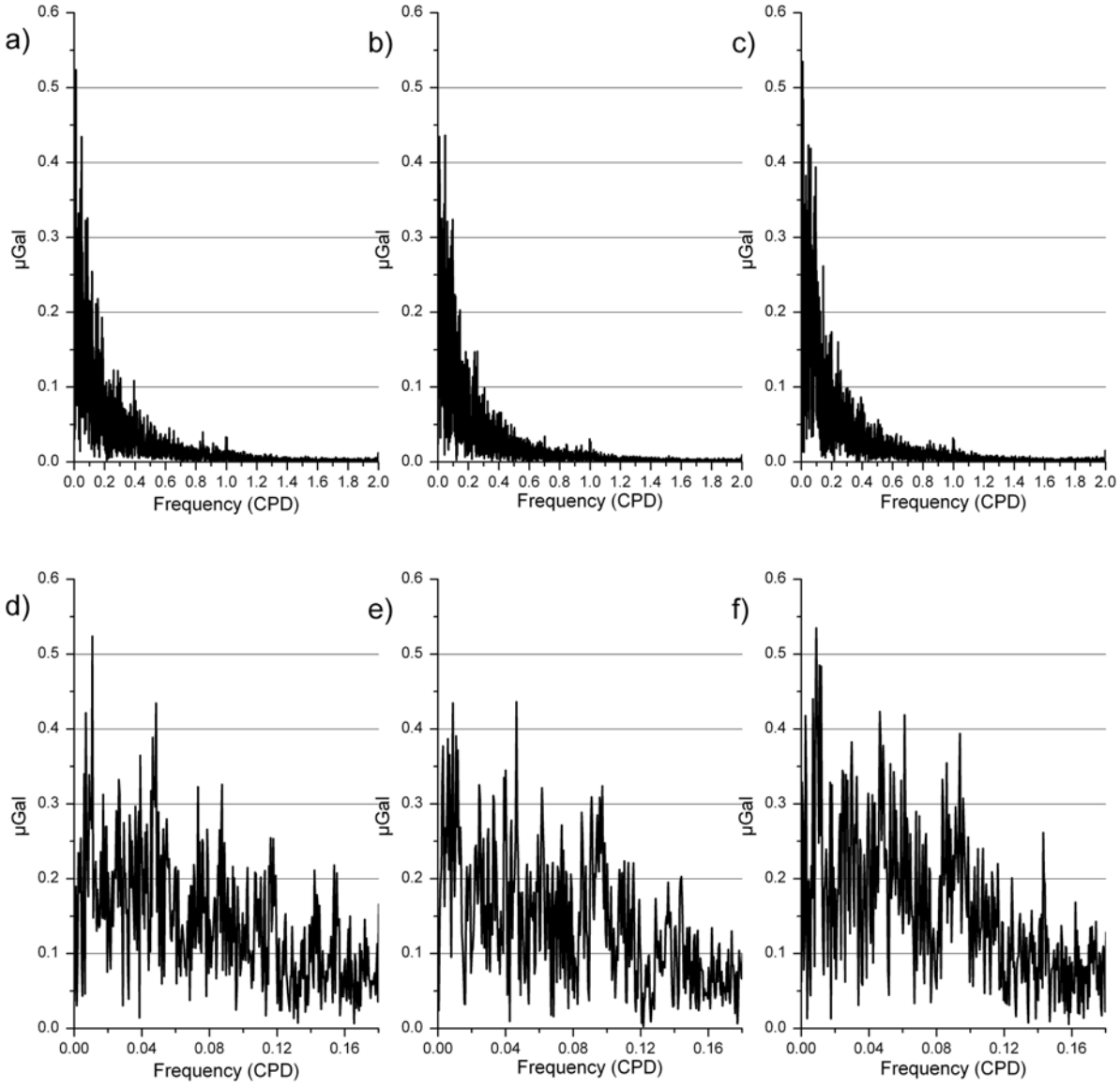

Figure 9
Amplitude spectra of different atmospheric effects from 2004/01/01 to 2007/12/31
a) reduction 3D+2D , b) reduction 2D data , c) admittance factor
enlarged
d) reduction 3D+2D , e) reduction 2D data , f) admittance factor

Fig.9a, b, c show the amplitude spectra of the reductions using (3D+2D) data, 2D data, and an admittance factor respectively. The amplitudes of the reduction based on 2D data have a 6% smaller value than the reduction based on (3D+2D) data and are 12% smaller than the reduction using an admittance factor on average in the spectral range between 0 and 2.0 CPD. To investigate in particular the range of long-period tides, the range between 0.0 and 0.18 CPD is enlarged (Fig.9d, e, f). The amplitude of the reduction using 2D data is 1.3% smaller than the reduction using (3D+2D) and 12% smaller than the reduction using an admittance factor in this range on average. The amplitude difference

between the reduction based on (3D+2D) data and 2D data in the range of long-period tides (1.3%) is smaller than that in the range between 0 and 2.0 CPD (6%). These differences in the amplitudes are seen in the gravity residuals after carrying out the tidal analysis, due to the fact that either a too large or too small atmospheric reduction is applied to the gravity data.

3-3 Result of tidal analysis

It is also investigated how the different atmospheric reductions affect the tidal analysis. The tidal analyses are carried out using "BAYTAP-G and -L" (Tamura et al., 1991). The data cover 3 years. For the analysis, the atmospheric reductions derived from the ECMWF data are interpolated to 1h sample. In order to analyze the long-period Earth tides using BAYTAP-L, the data are re-sampled to 1 day interval.

Fig.10a shows the SG data from Moxa station after removing steps and spikes from 1st of January, 2004 to 31st of December, 2006. The SG data have a peak-to-peak amplitude of 250μGal. Fig.10 b, c, d) show the gravity residuals after applying the three atmospheric reductions discussed before. Additionally the Earth tides, which are computed using different tidal factors determined after application of different pressure corrections as well as polar motion correction, are removed from the gravity observations. We calculate polar motion with IERS (International Earth Rotation Service) data using the well-known formula (IAGBN, 1992)

$$\delta g = -\delta \times 10^8 \times \omega^2 \times a \times 2 \times \sin\varphi\cos\varphi \cdot (x\cos\lambda - y\sin\lambda)\,\mu\text{Gal.} \quad (9)$$

where δg is gravity variation caused by polar motion , δ is 1.164 for the spherical elastic Earth, x and y (rad) are the coordinates from IERS , ω is Earth's rotational velocity (7292115×10^{-11} (rad/s)), a is equatorial radius (semi-major axis) of reference ellipsoid (6378136.3(m)), and ϕ and λ are respectively latitude and longitude of the observation site. In order to subtract the SA and SSA tide, the theoretical model of DDW (Dehant et al., 1999) is used.

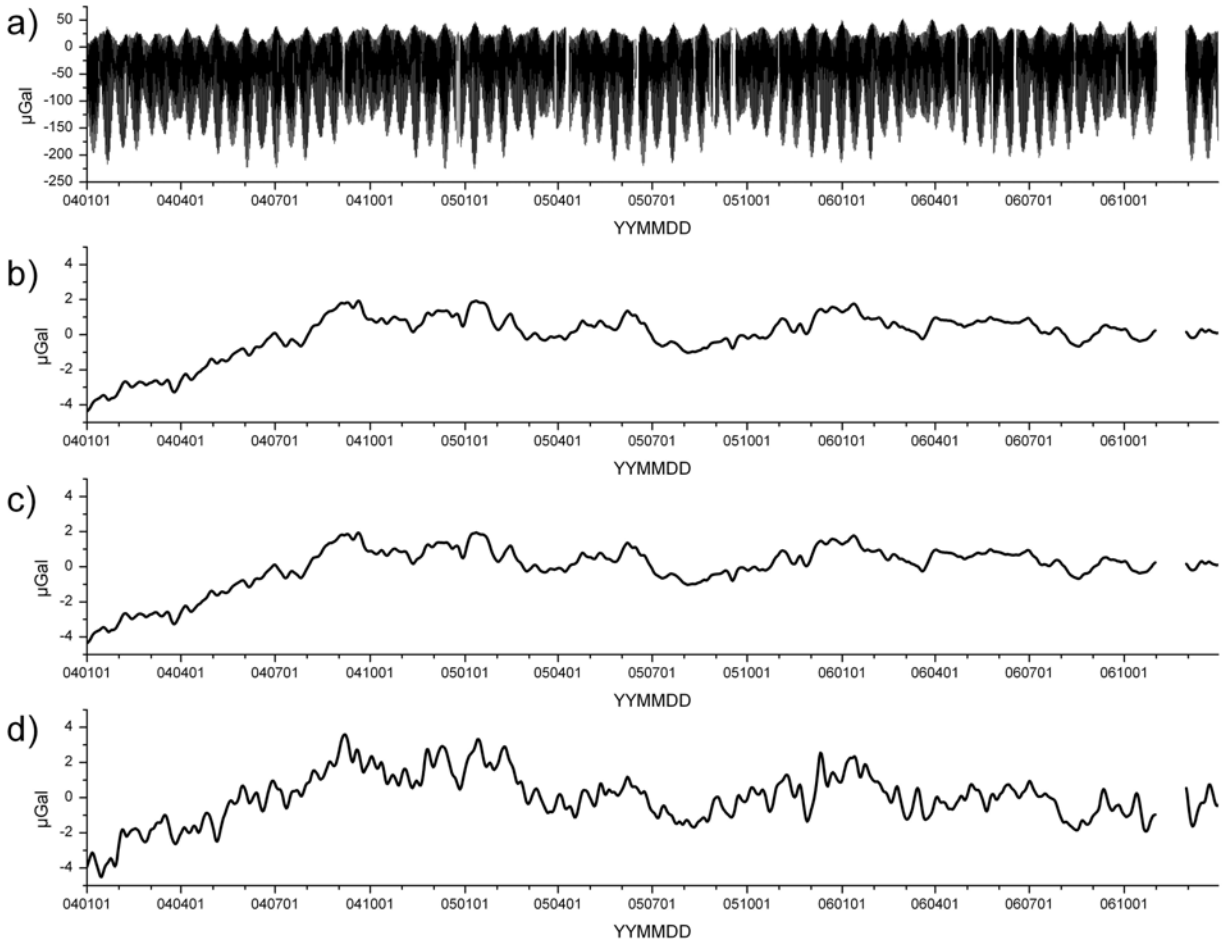

Figure 10
SG observation and gravity residuals from Moxa station after removing tides and atmospheric effect using different reductions from 2004/01/01 to 2006/12/31
a) SG data (after removing steps & disturbances)
b) reduction 3D+2D , c) reduction 2D data , d) admittance factor

The two reductions (Fig.10b, c) based on a physical approach yield similar gravity residual variations with a peak-to-peak amplitude of 7 µGal. The gravity residuals obtained by using an admittance factor (Fig.10d) contain stronger variations with a peak-to-peak amplitude of 1-3 µGal with periods of 5 days to 30 days which do not occur for the other two reductions.

In order to investigate in which period bands differences occur, Table 1 shows the mean amplitude of the gravity residuals after applying different atmospheric reductions for five period bands; periods longer than 1000 days, between 1000 and 250 days, between 250 and 50 days, between 50 and 15 days and 15 and 2 days.

Period bands		µGal	difference (%)		µGal	difference (%)
1000 d < T	2D data	0.3894	26.81	2D+temp data	0.2930	0.0025
	(3D+2D) data	0.3071		(3D+(2D+temp)) data	0.2937	
	admittance	0.3695		admittance	0.3695	
250 d < T < 1000 d	2D data	0.1924	-18.31	2D+temp data	0.2506	0.0045
	(3D+2D) data	0.2356		(3D+(2D+temp)) data	0.2495	
	admittance	0.4028		admittance	0.4028	
50 d < T < 250 d	2D data	0.0945	3.30	2D+temp data	0.0914	0.0026
	(3D+2D) data	0.0914		(3D+(2D+temp)) data	0.0911	
	admittance	0.1248		admittance	0.1248	
15 d < T < 50 d	2D data	0.0281	1.02	2D+temp data	0.0288	≈
	(3D+2D) data	0.0278		(3D+(2D+temp)) data	0.0288	
	admittance	0.0544		admittance	0.0544	
2 d < T < 15 d	2D data	0.0010	≈	2D+temp data	0.0013	≈
	(3D+2D) data	0.0010		(3D+(2D+temp)) data	0.0013	
	admittance	0.0034		admittance	0.0034	

Table 1
Mean amplitude of gravity residuals for reductions based on (3D+2D) data, 2D data (with and without temperature-dependent part) and an admittance factor for different period bands and difference between the physical approaches (%)

For comparison, results derived from the 2D- reduction without temperature variations are also shown in the table 1. If the temperature effects are not included, the gravity residuals applying the reduction based on (3D+2D) data is 1 - 3% different from the gravity residuals based on 2D data in the period band between 15 and 250 days on average. In the period band between 250 days and 1000 days, 18% of deviations exist between the gravity residuals based on the physical approaches. This result indicates that the reduction based on 2D data removes not only the signal related to the atmosphere in this period band but also other signal. However, if we include the temperature-dependent component, the differences between reductions using 3D data and 2D data become nearly zero. The application of an admittance factor leads to 1.2 - 3.4 times larger amplitudes than the other two methods in the considered five period bands. An explanation for this is that the spatial and temporal scale of air mass movements is more or less proportional (Fortak, 1971), for instance if the scale of the atmospheric mass movement is 1 km, then the associated temporal variation is in the range from 50 sec to 8 min, but if the spatial scale of atmosphere is 500 km, then the temporal variation is about 3 h to 8 days. With increasing spatial extension of an atmospheric mass, the deformation component increases, thus more of the attraction part is compensated. This in turn results in a reduced admittance factor for lower frequencies. Applying an admittance factor which is determined from short-period tides therefore leads to a well known too big

reduction in the long-period tides range. This explains why the amplitude of the reduction using an admittance factor is larger than the other two and the amplitude spectra of the reduction using an admittance factor is 11% - 12% larger than the others in the spectral range of long-period Earth tides.

Concerning the result of the tidal analyses, the sampling rate of the ECMWF data is 6 h, therefore, only the long-period tidal parameters are discussed. The amplitude factors using physical approaches do not have large discrepancies. All tidal factors and phases derived from the physical approaches are in agreement within the error bars of (3D+2D).

Concerning the amplitude factors between the reduction using (3D+2D) and using an admittance factor, the amplitude factor of MM, MF, MSTM and MSQM are not in agreement within the error bars of (3D+2D). The error values of the reduction based on an admittance factor are 44 - 73% larger than that of the reduction using (3D+2D) data.

For the differences between the phase values using (3D+2D) data and using an admittance factor, MM, MF and MSQM are not in agreement within the error bars of (3D+2D). The error bars of the reduction using an admittance factor have 42% - 72% larger than the reduction using (3D+2D) data.

Finally, table 2 shows the amplitude factor of the polar motion signal. This factor is estimated between the theoretical gravity polar motion signal, which is determined by use of equation 9 with δ=1.0, and the gravity residuals after applying the different atmospheric reductions, removing the tides and drifts. There is a 1.5% difference between the value of the factor after applying the reductions using 2D data including temperature and 3D data, however, these differences are within the associated standard deviation.

atmospheric reduction	amplitude factor	standard deviation
(3D+(2D+temp))	1.147	0.017
2D+temp	1.164	0.017
(3D+2D)	1.147	0.017
2D	1.165	0.017
admittance	1.159	0.023

Table 2
Amplitude factor of the polar motion signal derived after applying different atmospheric reductions

4, Conclusions

From computing the attraction effect of 6 zones up to 15° from Moxa station using 3D data from ECMWF and comparing it with the attraction effect derived

from 2D data (pressure and temperature) and a standard atmosphere, we find that the difference in the attraction effect from the zone up to 0.5° around the station, the ring-shaped zone of 0.5° - 1.5°, 1.5° - 3°, and 3° - 5° are respectively 4.5 μGal, 3 μGal, 0.8 μGal and 0.26 μGal. In contrast, the differences from the ring-shaped zone of 5° - 10° and 10° - 15° is below 0.2 μGal. We infer, therefore, that it makes sense to calculate atmospheric attraction effect up to 5° using 3D data

The difference between the physical reductions and the use of an admittance factor amounts to around 3 μGal with a RMS value of 0.4 μGal in a time span of 4 years and the differences between both physical approaches have a peak-to-peak amplitude of 0.5 μGal including seasonal variations with an amplitude of 0.15 μGal and a RMS value of 0.1 μGal.

From spectral analysis of these three reductions, it emerges that in the spectral range between 0.0 CPD and 0.18 CPD, the amplitude of the reduction using (3D+2D) data is 12% smaller than that of the reduction using an admittance factor on average and 1.3% larger than that of the reduction using 2D data (pressure and temperature). Moreover, in the spectral range between 0.0 to 2.0 CPD, the difference between the reduction using (3D+2D) data and 2D data becomes larger (6%). On the other hand, the difference between the reduction using (3D+2D) and an admittance factor is nearly the same value (12%).

Concerning the tidal analysis, the error bars of the reduction based on an admittance factor are 44% - 73% for the tidal factors and 42% - 72% for the phases larger than the reduction using (3D+2D) data by comparing the results. However, there are no visible improvements between the results based on the physical approaches.

Comparing the mean amplitude of the gravity residuals for five different period bands yields also no dramatic differences between the two physical reductions. If we do not consider the temperature-dependent component in the reduction using 2D data, there are 18% differences between both data sets. Moreover, we show that the amplitude of the residuals after a reduction using an admittance factor is 1.2 - 3.4 times larger than for the other two methods in the five period bands. This is explained by the fact that the impact of atmosphere cannot be represented using only one admittance factor for all frequencies due to the different spatial extensions of air masses and the associated velocities. This emphasises once more the findings by Warburton and Goodkind (1977), Crossley et al. (1995) and Neumeyer (1995). The reductions using (3D+2D) data or 2D data do not have this problem because they can be estimated directly using the atmospheric cells. The reductions derived from physical approaches capture the atmospheric effects better than the reduction derived from an admittance factor.

With regard to the development of an improved reduction on a physical basis, the consideration of 3D data and 2D data with a temperature-dependent component leads almost to the same result in the tidal analysis. A 1.5% difference exists between both physical approaches considering temperature variations in the determination of the amplitude factor of the polar motion signal.

The effect of actual vertical atmospheric distribution is not obvious; however, this accuracy is necessary for further studies of small long-period geodynamic signals such as the polar motion or long-period non-tidal mass shifts in the

oceans. The effect has a peak-to-peak amplitude of 2.2-2.7 μGal (Kroner et al. 2009). A reduction model should be at least one order of magnitude more accurate than the effect which is to be investigated. Therefore, it is recommended to use the more sophisticated atmospheric reduction model discussed in this paper.

Acknowledgements

We are grateful to the European Centere for Medium-Range Weather Forecasts (ECMWF) for providing the data. We thank Dr. Torsten Schmidt of GeoForschungsZentrum Potsdam for assisting with ECMWF data and Moxa observatory for supplying the barometric pressure and gravity data. Our thanks also go to anonymous reviewers for their valuable comments which lead a significant improvement of the paper.

This research is supported by the German Research Foundation by grant NE140911-1.

References

Boy, J.P., Hinderer, J., Gegout, P.,1998. Global atmospheric loading and gravity. Phys. Earth Planet. Int., **109**,161-177.

Boy, J.P., Gegout, P., Hinderer, J., 2002. Reduction of surface gravity from global atmospheric pressure loading. Geophys. J. Int., **149**, 534-545.

Crossley, D., Jensen O.G., Hinderer J., 1995. Effective barometric admittance and gravity residuals. Phys. Earth Planet. Int., **90**, 221-241.

Crossley, D., Hinderer, J., Casula, G., Francis, O., Hsu, H.T., Imanishi, Y., Jentzsch, G., Kääriänen, J., Merriam, J., Meurers, B., Neumeyer J., Richter, B., Shibuya, K., Sato, T., 1999. Network of superconducting gravimeters benefits a number of disciplines, EOS, Trans. Am. Geophys. U., **80**, 121-126.

Dehant, V., Defraigne, P., Wahr, J.M., 1999. Tides for a convective Earth, J. Geophys. Res, **104**, 1035-1058.

ECMWF, Higher resolution model upgrade - 2 February 2006, Operational upgrades.

Farrell, W.E., 1972. Deformation of the Earth by surface loads.Rev. Geophys. Space Phys., **10**, 761–797.

Fortak, H., 1971. Meteorologie. Carl Hebel Verlagsbuchhandlung, Berlin and Darmstadt.

Guo, J. Y., Li, B. Y., Huang, Y., Deng, T. H., Xu., Q. S. and Ning, S. J., 2004. Green's function of the deformation of the Earth as a result of atmospheric loading. Geophys. J. Int., **159**, 53-69.

IAGBN,1992. Absolute Observations Data Processing Standards.

Kroner, C. & Jentzsch, G., 1999. Comparison of different barometric pressure reductions for gravity data and resulting consequences. Phys. Earth Planet. Int., **115**, 205-218.

Kroner, C., Jahr, Th., Jentzsch, G., 2004. Results from 44 months of observations with a superconducting gravimeter at Moxa/Germany. Journal of Geodynamics, **38**, 263-280.

Kroner, C., Thomas, M., Dobslaw, H., Abe, M., Weise, A., 2009. Effect of non-tidal mass shifts on observations with superconducting gravimeters. Journal of Geodynamics., accepted.

Merriam, J.B., 1992. Atmospheric pressure and gravity. Geophys. J. Int., **109,** 488-500.

NASA (National aeronautics and Space Administration) U.S. Standard Atmosphere, 1976, U.S. Government Printing Office, Washington, D.C., 1976.

Neumeyer, J., 1995. Frequency dependent atmospheric pressure correction on gravity variations by means of cross spectral analysis. Bulletin d'Information des Marées Terrestres, **122**, 9212-9220.

Neumeyer, J., Hagedoorn, J., Leitloff, J., Schmidt, T., 2004. Gravity reduction with three-dimensional atmospheric pressure data for precise ground gravity measurements. Journal of Geodynamics, **38**, 437-450.

Neumeyer, J., Schmidt, T., Stoeber, C., 2006. Improved determination of the atmospheric attraction with 3D air density data and its reduction on ground gravity measurements. Dynamic Planet - monitoring and understanding a dynamic planet with geodetic and oceanographic tools ; IAG Symposium, Cairns, Australia, 22-26 August, 2005 - International Association of Geodesy Symposia, **130**, 541-548.

Sun, H.-P., Ducarme, B., Dehant, V., 1995. Theoretical calculation of atmospheric gravity Green's functions. Proc. 2nd Workshop on non tidal gravity changes, intercomparison between absolute and superconducting gravimeters', Cahiers du Centre Européen de Géodynamique et de Séismologie, **11**, 223-237.

Tamura, Y., Sato, T., Ooe, M., Ishiguro, M., 1991. A procedure for tidal analysis with a Bayesian information criterion. Geophys. J. Int., **104**, 507-516.

Warburton R. J. & Goodkind J. M., 1977. The influence of barometric - pressure variations on gravity. Geophys. J. R. Astr. Soc., **48**, 281-292.